Higher-order graph wavelets and sparsity on circulant graphs

Madeleine S. Kotzagiannidis and Pier Luigi Dragotti
Department of Electrical and Electronic Engineering
Imperial College London, United Kingdom

ABSTRACT

The notion of a graph wavelet gives rise to more advanced processing of data on graphs due to its ability to operate in a localized manner, across newly arising data-dependency structures, with respect to the graph signal and underlying graph structure, thereby taking into consideration the inherent geometry of the data. In this work, we tackle the problem of creating graph wavelet filterbanks on circulant graphs for a sparse representation of certain classes of graph signals. The underlying graph can hereby be data-driven as well as fixed, for applications including image processing and social network theory, whereby clusters can be modelled as circulant graphs, respectively. We present a set of novel graph wavelet filterbank constructions, which annihilate higher-order polynomial graph signals (up to a border effect) defined on the vertices of undirected, circulant graphs, and are localised in the vertex domain. We give preliminary results on their performance for non-linear graph signal approximation and denoising. Furthermore, we provide extensions to our previously developed segmentation-inspired graph wavelet framework for non-linear image approximation, by incorporating notions of smoothness and vanishing moments, which further improve performance compared to traditional methods.

Keywords: Signal processing on graphs, graph wavelet, circulant graph, sparsity

1. INTRODUCTION

A breadth of recent contributions encompassing the ascendent field of graph signal processing, inspired by the potential of graphs to capture complex information beyond the classical domain, has extended traditional signal processing to the higher-dimensional graph domain by establishing equivalencies, while taking advantage of newly arising data dependencies.[1] Wavelets on graphs, in particular, facilitate advanced (and potentially superior) processing of given data, which is captured in graph signals and the corresponding (often data-driven) underlying graphs, through localized operations with respect to the inherent geometry of the data, thereby constituting an intriguing extension of classical wavelet theory. Proposed designs such as the diffusion wavelet,[2] the perfect reconstruction filterbank on bipartite graphs,[3] and the spectral graph wavelet,[4] with an ensuing discussion of sparsity on graphs,[5] have been tailored to satisfy a (sub-)set of various desirable properties, including, but not limited to, compact support in the vertex domain, invertibility, and critical sampling.

The objective of this work is to achieve a sparse graph wavelet representation, for the realisation of a superior non-linear approximation performance on graphs. Hereby, we derive a selection of graph wavelet constructions, localized in the graph-vertex domain, which annihilate higher-order 'polynomial' graph signals on undirected circulant graphs. The latter represent an appealing class of graphs to operate on, due to a set of properties, which facilitate downsampling and shifting operations.[6] Not least of all, circulant graphs provide an immediate connection to the traditional signal processing domain due to the fact that circulant matrices are diagonalizable by the DFT-matrix.

The spline-like graph wavelet filterbank on circulant graphs, introduced by Ekambaram et al.,[7] which inspired our current design, while localized in the vertex domain, only annihilates up to linear polynomial graph signals. To the best of our knowledge, there does not exist a comparable graph wavelet construction on circulant graphs, which is tailored to the annihilation of higher-order polynomial graph signals.

Further author information:
E-mail: {m.kotzagiannidis13, p.dragotti}@imperial.ac.uk

Based on a generalization of the annihilation property of the graph Laplacian matrix, whose associated polynomial function, as we will proceed to demonstrate, has two vanishing moments for a sufficiently small bandwidth, we explore the design of graph wavelet filterbanks on undirected circulant graphs; in particular, we consider constructions tailored to data-driven graphs (such as for image processing) as well as constructions for scenarios where the underlying graph model is fixed and/or independent of the graph signal, such as social networks.

In our prior work,[8] we have shown that the application of the existing spline-like circulant graph wavelets[6,7] within our proposed, graph-cut inspired scheme to the graph-realisation of a 2D image leads to superior performance in non-linear image approximation than traditional 2D transforms. We additionally present refinements of this scheme, by incorporating a node relabelling step which aims to minimize the total variation of the graph signal as well as the bandwidth of the associated graph wavelet matrix for a maximum sparse representation.

This paper is organized as follows: in Section 2, we present preliminaries, followed, in Sections 3 and 4, by the introduction of our higher-order graph wavelet filterbank constructions. Extensions to image processing on graphs are discussed in Section 5, also including experimental results, and we give concluding remarks and an outlook on future work in Section 6.

2. PRELIMINARIES

A graph $G = (V, E)$ is defined by a vertex set V, of cardinality $|V| = N$, and an edge set E, and throughout this work, we primarily focus on graphs that are undirected, connected, weighted, and do not contain self-loops. The connectedness of G is represented via an adjacency matrix $\mathbf{A}$, whose entries are $a_{i,j} \neq 0$ if there exists an edge between vertices i and j, and $a_{i,j} = 0$ otherwise, and a diagonal degree matrix $\mathbf{D}$, with entries $d_{i,i} = \sum_j a_{i,j}$.

The (non-normalized) graph Laplacian matrix $\mathbf{L} = \mathbf{D} - \mathbf{A}$, is positive semi-definite, and therefore has a complete set of orthonormal eigenvectors $\{\mathbf{u}_l\}_{l=0}^{N-1}$, with corresponding non-negative eigenvalues $\{\lambda_l\}_{l=0}^{N-1}$. We denote a graph signal $\mathbf{x}$, which is a real-valued scalar function defined on the vertices of a graph G, as a vector $\mathbf{x} \in \mathbb{R}^N$, with value $x(i)$ at node i. The Graph Fourier Transform (GFT) of $\mathbf{x}$ is defined as: $\mathbf{X}^G = \mathbf{U}^H \mathbf{x}$, with $\mathbf{U} = [\mathbf{u}_0|...|\mathbf{u}_{N-1}]$, where H denotes the Hermitian transpose.

The class of circulant graphs, formally defined as graphs with generating set $S = \{s_k\}_{k=1}^P$, whose elements $0 < s_k \leq N-1$ determine an edge between the node pair $(i, (i+s_k)_{modN})$, or in simplified terms, the class of graphs whose adjacency matrix is circulant (see Figure 1 for examples), has been shown to facilitate the development of particularly convenient concepts and operations in graph signal processing, ranging from downsampling operations to graph filterbank constructions.[6,7,9] In particular, the spline-like graph wavelet filterbank poses an interesting graph-generalization of the traditional simple spline:

Definition 1. The spline-like graph wavelet filterbank, comprising the following low-and high-pass filters

$$\mathbf{H}_{LP} = \frac{1}{2}\left(\mathbf{I}_N + \frac{\mathbf{A}}{d}\right) \tag{1}$$

$$\mathbf{H}_{HP} = \frac{1}{2}\left(\mathbf{I}_N - \frac{\mathbf{A}}{d}\right) \tag{2}$$

where $\mathbf{A}$ is the adjacency matrix of an undirected, connected and circulant graph and d the degree per node, is invertible as long as at least one node retains the low-pass component.[7]

Hereby, the downsampling operation can be conducted with respect to any element of the generating set S.[6] In this paper, however, unless indicated otherwise, we choose to adhere to the standard downsampling by 2 with respect to the outmost cycle of the graph (i.e. with respect to $s_1 = 1 \in S$) for even N, whereby every other labelled node is skipped, and assume that the graph in question is connected, for simplicity.

Furthermore, we can define the symmetric, circulant graph Laplacian matrix $\mathbf{L}$, with first row $[l_0 \quad ... \quad l_{N-1}]$, via its representer polynomial $l(z) = \sum_{i=0}^{N-1} l_i z^i$; in particular, for the circulant permutation matrix $\mathbf{\Pi}$ with first row $[0 \quad 1 \quad 0 \quad ...]$, we obtain $\mathbf{L} = \sum_{i=0}^{N-1} l_i \mathbf{\Pi}^i$.

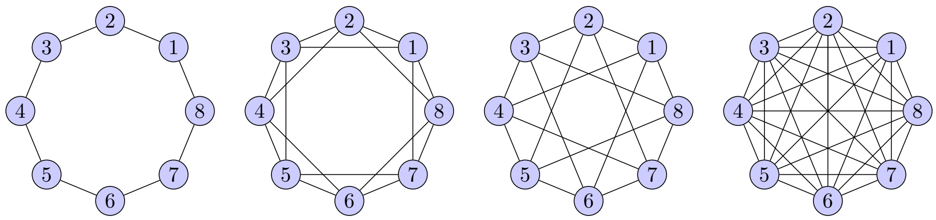

Figure 1. Circulant Graphs with generating sets $S = \{1\}$, $S = \{1, 2\}$, $S = \{1, 3\}$ and $S = \{1, 2, 3, 4\}$ (f. left)

3. THE GRAPH LAPLACIAN AS A HIGH-PASS FILTER

It has been observed[9] that the graph Laplacian matrix carries the notion of a high-pass filter, by annihilating constant graph signals via its weighted difference operation; furthermore it is well known that the localized filtering operation in the graph vertex domain can be defined as a polynomial in the graph Laplacian matrix acting on a graph signal.[1] In light of this, we introduce the following interesting result pertaining to the graph Laplacian matrix of circulant graphs in particular:

Lemma 1. For an undirected, circulant graph $G = (V, E)$ of dimension N, the associated representer polynomial $l(z) = l_0 + \sum_{i=1}^{M} l_i(z^i + z^{-i})$ of the graph Laplacian matrix $\mathbf{L} = \mathbf{D} - \mathbf{A}$, with first row $[l_0\ l_1\ l_2\ \ \ ...\ \ \ l_2\ l_1]$, has two vanishing moments. Therefore, the operator $\mathbf{L}$ annihilates polynomial graph signals of up to degree $n = 1$, subject to a border effect determined by the bandwidth M of $\mathbf{L}$, whereby $M << N$.

Proof: Consider the polynomial representation of the first row of the graph Laplacian matrix with degree $d = \sum_{i=1}^{M} 2d_i$ per node and symmetric weights d_i:

$$l(z) = (-d_M z^{-M} - ... - d_1 z^{-1} + d - d_1 z - ... - d_M z^M) = \sum_{i=1}^{M} d_i (z^i - 1)(z^{-i} - 1),$$

whereby M is the bandwidth of $\mathbf{L}$. We observe that the factors on the RHS are divisible by $(z^{\pm 1} - 1)$ respectively, using the equality $z^n - 1 = (z - 1)(1 + z + ... + z^{n-1})$, thus proving that the representer polynomial associated with the matrix $\mathbf{L}$ has two vanishing moments.
Therefore, if the adjacency matrix of G is a symmetric, banded circulant matrix of bandwidth M, the corresponding graph Laplacian matrix $\mathbf{L}$ annihilates linear polynomial graph signals on the graph G up to the boundary effect; the latter increases with parameter M, thus requiring M to be sufficiently small with respect to the dimension N of G.

4. HIGHER-ORDER GRAPH WAVELETS

In the following, we present a breadth of design options for the construction of higher-order graph wavelet filterbanks, which take advantage of the previously introduced annihilation property of the graph Laplacian matrix $\mathbf{L}$. We begin by extending the spline-like graph wavelet filterbank in Eqs. (1-2), whose high pass-filter is conveniently given by the normalized $\mathbf{L}$, to higher order by raising it to the k-th power.

Proposition 1. Given the undirected, and connected circulant graph $G = (V, E)$ of dimension N, with adjacency matrix $\mathbf{A}$ and degree d per node, we define the higher-order graph-spline wavelet transform (HGSWT), composed of the low-and high-pass filters

$$\mathbf{H}_{LP} = \frac{1}{2^k} \left(\mathbf{I}_N + \frac{\mathbf{A}}{d} \right)^k \tag{3}$$

$$\mathbf{H}_{HP} = \frac{1}{2^k} \left(\mathbf{I}_N - \frac{\mathbf{A}}{d} \right)^k \tag{4}$$

whose associated 'high-pass' polynomial function $h_{HP}(z)$ has $2k$ vanishing moments. This filterbank is invertible for any downsampling pattern, as long as at least one node retains the low-pass component.

Proof: It is evident that if the polynomial representation $l(z)$ of graph Laplacian $\mathbf{L}$ has 2 vanishing moments, the function $h_{HP}(z) = \frac{l(z)^k}{(2d)^k}$ associated with $\mathbf{L}^k$ will have $2k$ vanishing moments due to the equivalency between polynomial and circulant matrix multiplication, generalizing the annihilation property to higher order; thus we proceed to demonstrate invertibility of the above filterbank. The core of the proof follows a similar line of argumentation as the one provided in Ref. 9 for $k = 1$ with generalizations pertaining to the parameter k; for completeness we present it here in its entirety.
By the binomial theorem, we have

$$\frac{1}{2^k}\left(\mathbf{I}_N + \frac{\mathbf{A}}{d}\right)^k = \frac{1}{2^k}\sum_{j=0}^{k}\binom{k}{j}\left(\frac{\mathbf{A}}{d}\right)^j$$

and we need to demonstrate that the nullspace of the filterbank (after downsampling)

$$\frac{1}{2^k}\left(\sum_{j=0}\binom{k}{2j}\left(\frac{\mathbf{A}}{d}\right)^{2j} + \mathbf{K}\sum_{j=0}\binom{k}{2j+1}\left(\frac{\mathbf{A}}{d}\right)^{2j+1}\right)$$

is empty, where $\mathbf{K}$ is the diagonal downsampling matrix with entries $K(i,i) = \pm 1$ if node i retains the low- or high-pass component. Assume the contrary by letting a vector $\mathbf{z} = \mathbf{Vr}$ lie in the nullspace:

$$\frac{1}{2^k}\left(\sum_{j=0}\binom{k}{2j}\left(\frac{\mathbf{A}}{d}\right)^{2j} + \mathbf{K}\sum_{j=0}\binom{k}{2j+1}\left(\frac{\mathbf{A}}{d}\right)^{2j+1}\right)\mathbf{Vr} = \mathbf{0}_N \tag{5}$$

$$||\mathbf{V}\sum_{j=0}\binom{k}{2j}\mathbf{\Gamma}^{2j}\mathbf{r}||^2 = ||\mathbf{KV}\sum_{j=0}\binom{k}{2j+1}\mathbf{\Gamma}^{2j+1}\mathbf{r}||^2 \tag{6}$$

where Eq. (6) results from the eigendecomposition $\mathbf{V}\mathbf{\Gamma}^j\mathbf{V}^H = \left(\frac{\mathbf{A}}{d}\right)^j$ and subsequently taking the l_2-vector norm of both sides of the rearranged equation. At last, we obtain

$$\sum_{i=0}^{N-1} r(i)^2\left(\left(\sum_{j=0}\binom{k}{2j}\gamma_i^{2j}\right)^2 - \left(\sum_{j=0}\binom{k}{2j+1}\gamma_i^{2j+1}\right)^2\right) \overset{(a)}{=} \sum_{i=0}^{N-1} r(i)^2(B_i^2 - A_i^2) = 0, \tag{7}$$

whereby in (a), we let A_i and B_i represent the sum of odd and even terms in the binomial series respectively. For the nullspace to be empty, we need to show that $\mathbf{r} = \mathbf{0}_N$, or $(B_i^2 - A_i^2) \neq 0$. By utilizing the fact that for a general binomial series $(x+a)^n$, with terms A_i and B_i, the following holds: $(x^2 - a^2)^n = A_i^2 - B_i^2$, we obtain

$$\sum_{i=0}^{N-1} r(i)^2(B_i^2 - A_i^2) = \sum_{i=0}^{N-1} r(i)^2(\gamma_i^2 - 1)^k = 0.$$

Since the eigenvalues of the normalized, Hermitian adjacency matrix $\frac{\mathbf{A}}{d}$ are given by $|\gamma_i| \leq 1$,[10] where $\gamma = -1$ exists only if the graph is bipartite, we have that $|r(i)| > 0$ only if $|\gamma_i| = 1$ and $r(i) = 0$ otherwise. Thus, we let $\mathbf{z} = \frac{r(0)}{\sqrt{N}}\mathbf{1}_N + \tilde{\mathbf{V}}\mathbf{r}$, with $\tilde{\mathbf{V}}$ being the set of eigenvectors of $\gamma = -1$ and $\frac{r(0)}{\sqrt{N}}\mathbf{1}_N$ corresponding to $\gamma = 1$. We consider the case of a non-bipartite graph first:

$$\frac{r(0)}{\sqrt{N}}\left(\sum_{j=0}\binom{k}{2j}\mathbf{1}_N + \mathbf{K}\sum_{j=0}\binom{k}{2j+1}\mathbf{1}_N\right) = \mathbf{0}_N$$

Since $\sum_{j=0}\binom{k}{2j}=\sum_{j=0}\binom{k}{2j+1}$, we need at least one entry $K(i,i)=1$, such that $r(0)=0$.
In the bipartite case, due to spectral folding, if γ is an eigenvalue of $\mathbf{A}$ with eigenvector $[\mathbf{v}_B,\mathbf{v}_{B^C}]$, so is $-\gamma$ with eigenvector $[\mathbf{v}_B,-\mathbf{v}_{B^C}]$, where B is the set of the node indices in one bipartite set.[10] Then $\gamma=1$ and $\gamma=-1$ each have multiplicity one with respective eigenvectors $\mathbf{1}_N$ and $[\mathbf{1}_B,-\mathbf{1}_{B^C}]$, where $|B|=|B^C|=N/2$, giving

$$\frac{r(0)}{\sqrt{N}}\underbrace{\left(\sum_{j=0}\binom{k}{2j}\mathbf{I}_N+\mathbf{K}\sum_{j=0}\binom{k}{2j+1}\right)}_{T_1}\mathbf{1}_N+r(1)\underbrace{\left(\mathbf{I}_N\sum_{j=0}\binom{k}{2j}-\mathbf{K}\sum_{j=0}\binom{k}{2j+1}\right)}_{T_2}[\mathbf{1}_B,-\mathbf{1}_{B^C}]=\mathbf{0}_N. \quad (8)$$

Hereby we have used the property $\frac{\mathbf{A}}{d}\mathbf{v}=\gamma\mathbf{v}$, in $\left(\frac{\mathbf{A}}{d}\right)^j[\mathbf{1}_B,-\mathbf{1}_{B^C}]=(-1)^j[\mathbf{1}_B,-\mathbf{1}_{B^C}]$, leading to an alternating pattern when j is odd.
In particular, we note that for any choice of downsampling pattern $\mathbf{K}$, the terms T_1 and T_2 in the first and second summands respectively in Eq. (8), will have zero entries along the main diagonal, which lie in complementary index sets. Therefore, as long as at least one node retains the lowpass component $K(i,i)=1$, we have that $r(0)=0$ and $r(1)=0$, which again implies that $\mathbf{z}=\mathbf{0}$, completing the proof.

4.1 Complementary Graph Wavelets

A 1-D discrete-time signal can be represented as the graph signal defined on the vertices of a simple cycle, establishing a link between traditional and graph signal processing; hereby, we observe that the derived higher-order filterbank then produces the traditional higher-order splines obtained via convolution of the linear spline $\beta_1(t)=\beta_0(t)*\beta_0(t)$ with itself, where $\beta_0(t)$ is the box function.[11] We can extend this property to general circulant graphs, given that the corresponding graph wavelet matrices are circulant and diagonalizable by the DFT-matrix (the GFT-representation), while adding the higher-dimensional element given by the complex connectivity of such graphs.
While the filterbank introduced in Eqs. (3-4) is well-defined in the graph vertex domain via the analysis branch, it does not give rise to a concrete definition of the corresponding synthesis branch. Furthermore, we observe that while the high-pass filter can annihilate polynomial graph signals, the low-pass filter does not necessarily reproduce such (unless it is bipartite, i.e. the elements in S are odd). In addition, both analysis filters have compact support of the same length, while the synthesis filters are comparatively longer. This has motivated the development of a new class of graph wavelet filterbanks on circulant graphs, which make use of traditional spectral factorization techniques.

Let the analysis high-pass filter be given by the normalized graph Laplacian matrix $\mathbf{L}$ with the associated polynomial $H_1(z)=\frac{1}{(2d)^k}l(z)^k$, and let the synthesis low-pass filter be defined by the polynomial $G_0(z)=-z^{-1}H_1(-z)$. We derive the corresponding analysis low-pass filter $H_0(z)$ via spectral factorisation, whereby $P(z)=H_0(z)G_0(z)$ is subject to the constraint of the halfband condition $P(z)+P(-z)=2$.
In general, given the normalized higher-order (graph Laplacian) high-pass filter polynomial

$$H_1(z)=(0.5-d_1(z+z^{-1})-...-d_M(z^M+z^{-M}))^k,$$

we determine $H_0(z)$ by noting that $P(z)$ is a polynomial of odd powers, and setting the constraint that $H_0(z)=\sum_{i=0}^{N}r_i(z^i+z^{-i})$ be symmetric:

$$\left(0.5-\sum_{i=1}^{M}(-1)^i d_i(z^i+z^{-i})\right)^k\left(\sum_{i=0}^{N}r_i(z^i+z^{-i})\right)=1+\sum_{i=0}^{L}p_{2i+1}(z^{2i+1}+z^{-(2i+1)}).$$

In addition, we may further impose the restriction that the analysis and synthesis filters have an equal number of vanishing moments $2k$, by setting $H_0(z)=(z+1)^k(z^{-1}+1)^kR(z)$, where $R(z)$ is the polynomial to be determined. In the case of $k=1$, we require the highest degrees of each equation to be $2L+1=M+N$; as we have $L+1$ constraints $p_{2n}=0$, $n=1,...,L$, and $p_0=1$, and $N+1$ unknowns r_i, we require $L=N=\frac{M+N-1}{2}$, or $N=M-1$, leading to a linear system of equations with a unique solution.

In case of a higher-order filterbank with $k > 1$, the constraints change as follows: $N = L = \frac{Mk+N-1}{2}$, or $N = Mk - 1$. If we further impose that both synthesis and analysis filters have an equal number of vanishing moments, we need to include the additional term $(z+1)^k(z^{-1}+1)^k$ for $H_1(z) = \frac{1}{(2d)^k} l(z)^k$, and require $N = Mk + k - 1$. Hereby, the resulting graph wavelet filters are symmetric.

Proposition 2. Given the undirected, and connected circulant graph $G = (V, E)$ of dimension N, with adjacency matrix $\mathbf{A}$ and degree d per node, we define the higher-order 'complementary' graph-spline wavelet transform (HCGSWT) via the set of analysis filters:

$$\mathbf{H}_{LP,an} = \mathbf{C}\tilde{\mathbf{H}}_{LP} = \mathbf{C}\left(\mathbf{I}_N + \frac{\mathbf{A}}{d}\right)^k \tag{9}$$

$$\mathbf{H}_{HP,an} = \frac{1}{2^k}\left(\mathbf{I}_N - \frac{\mathbf{A}}{d}\right)^k \tag{10}$$

and the set of synthesis filters:

$$\mathbf{H}_{LP,syn} = c_1(\mathbf{H}_{HP,an}) \circ I_{HP} \tag{11}$$

$$\mathbf{H}_{HP,syn} = c_2(\mathbf{H}_{LP,an}) \circ I_{LP} \tag{12}$$

where $c_i, i \in \{1, 2\}$ are normalization coefficients, and $I_{LP/HP}$ are circulant indicator matrices, whose entries $\{1, -1\}$ coincide with those of $\mathbf{H}_{LP/HP,an}$.

Hereby, we note that the spread of the new lowpass filter $\mathbf{H}_{LP,an}$ in the vertex domain does not coincide exactly with the adjacency matrix of the graph, but rather encompasses a subset $\tilde{S}_i$ of vertices within the k-hop local neighborhood $N(i, k)$ of vertex $i \in V$, which we denote as a simple convolution operation between the polynomial representation of the circulant filter-like coefficient matrix $\mathbf{C}$ and the associated polynomial of the traditional lowpass-graph filter $\tilde{\mathbf{H}}_{LP}$ in Eq. (1); the latter is based on the adjacency matrix and is easily shown to be generally invertible (if G is non-bipartite). In addition, the set $\tilde{S}$ depends on the initial constraints we impose on $H_{LP,an}(z)$.
We further note that unlike the constructions in Eqs. (3-4), this type of filterbank facilitates only the standard alternating downsampling pattern on graphs with respect to $s = 1 \in S$, whereby every other node is skipped.

5. EXPERIMENTAL RESULTS

In the following, we distinguish between two major categories of possible applications for graph wavelets. On the one hand, these include scenarios for which the graph at hand is fixed and data-independent of the graph signal, and on the other hand, we consider scenarios for which the graph and corresponding graph signal are both data-driven, commonly used, for instance, for the representation of images.

5.1 Polynomial Signals on Graphs

We consider a fixed circulant graph $G = (V, E)$, whose adjacency matrix is of sufficiently small bandwidth M, and define a set of (piecewise) polynomial graph signals $P = \{\mathbf{p}_j\}_{j=1}^M$ to lie on the vertices of G, whereby $\mathbf{p}_j \in \mathbb{R}^N$ is the vectorized form of the discrete-time piecewise polynomial $p_j[n]$

$$p_j[n] = \sum_{i=0}^{K} \tilde{p}_i[n]\mathbf{1}_{[k_i,k_{i+1}]}[n], \quad n \in [0, N-1], \quad i = 0, ..., K$$

with $k_0 = 0$, and $k_{K+1} = N$, and $\tilde{p}_i[n]$ is a sampled polynomial of maximum degree D.
It becomes evident that the aforementioned set of graph signals can be highly compressible in the graph domain as well, given that we can achieve a sparse multiresolution representation in the graph wavelet domain by applying the proposed transforms iteratively on the low-pass branch. Amongst possible applications, we note for instance

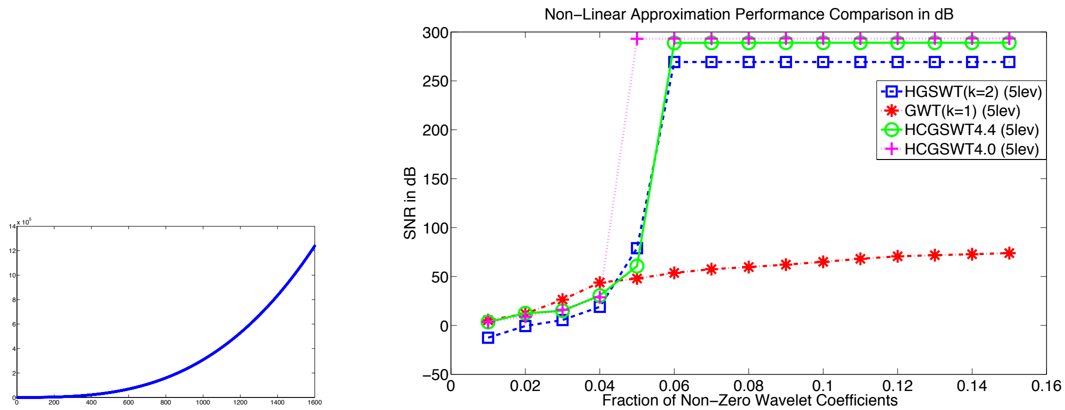

Figure 2. Non-Linear Approximation Performance Comparison between the regular GWT and proposed higher-order GWT on a fixed graph with $S = \{1, 2\}$ at 5 levels for a Cubic Graph Signal (left) with N=1600

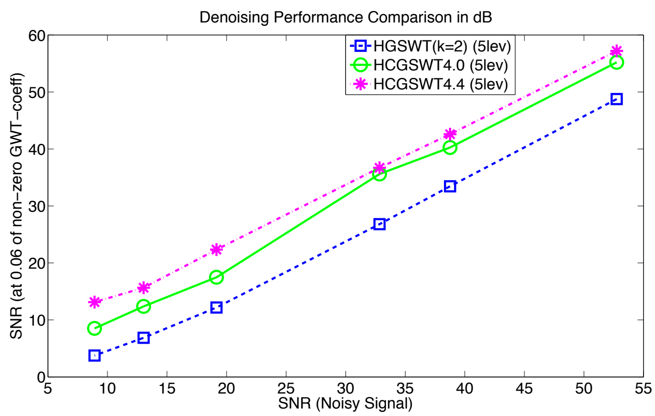

Figure 3. Denoising Performance Comparison between proposed higher-order GWT on a fixed graph with $S = \{1, 2\}$ at 5 levels for a Cubic Graph Signal with N=1600 (at 6% of highest magnitude GWT coefficients)

the analysis of suitable graph signals supported on graphs, modelling clusters in social networks. Hereby, we represent individual clusters as circulant sub-graphs (M-regular subgraphs, in particular), whose nodes exhibit similar neighborhoods, while the underlying graph signal(s) can be expressed in terms of and/or approximated by (piecewise) polynomials, yet are not necessarily smooth with respect to the graph.
In Figure 2, we compare the non-linear approximation performance between the exisiting (Eqs. (1-2)), and proposed (Eqs. (3-4) and (9-12)) graph wavelets of the same order ($k = 2$), and note that we can achieve perfect reconstruction for the latter at a small number of retained graph wavelet coefficients due to their higher-order sparsifying effect. In addition, we investigate the performance of the proposed constructions in the presence of noise, which reveals that the balanced construction with the same number of vanishing moments (4.4) at the analysis and synthesis branch performs best for the example at hand (see Figure 3). For both scenarios, we perform a multiscale decomposition at 5 levels, and reconnect edges in the graphs after downsampling such that they retain their original generating set S.

5.2 Graph Wavelets for Non-Linear Image Approximation

In prior work,[8] we considered the application of the spline-like GWT (see Eqs. (1-2)) (with 2 vanishing moments) to images. In particular, we constructed a graph G via a bilateral similarity measure based on the image at hand, whereby we let each node in G represent a pixel, and define the edge weights between the node pair (i, j) as

$$w_{i,j} = e^{-\frac{||p_i - p_j||_2^2}{\sigma_p^2}} e^{-\frac{|I(i)-I(j)|^2}{\sigma_I^2}}, \quad i, j, \in \{1, ..., N\}$$

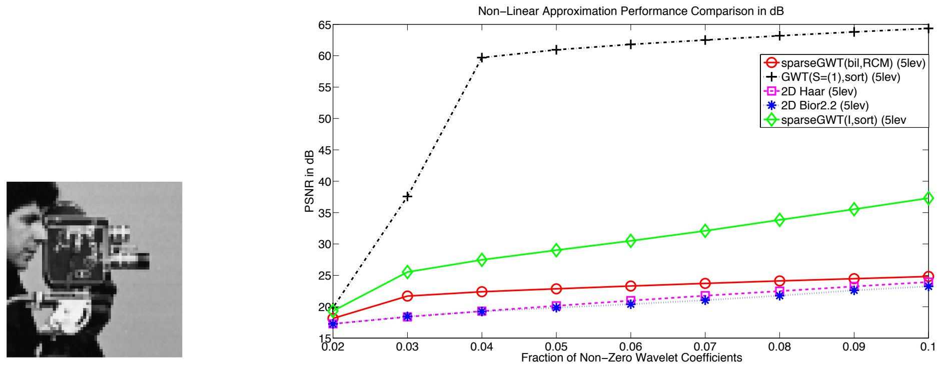

Figure 4. Non-Linear Approximation Performance Comparison between the 2D Haar, the 2D Linear Spline and a variety of proposed GWT at 5 levels on a 64×64 Image Patch from ‘cameraman’

for spatial and intensity parameters p and I. We subsequently proceed to conduct the graph wavelet analysis on smooth regions of the image, which are obtained by performing a graph cut[12] on G, and computing the nearest circulant graph-approximations $\tilde{G}_i$ of the individual subgraphs G_i, see Ref. 8 for a more detailed discussion. Hereby, we resorted to minimising the Frobenius-norm error[13] by averaging over the diagonals of a given, general matrix $\mathbf{A}$ to obtain its nearest circulant matrix approximation $\mathbf{C}$:

$$\mathbf{C} = \sum_{i=0}^{N-1} \frac{1}{N} \langle \mathbf{A}, \mathbf{\Pi}^i \rangle_F \mathbf{\Pi}^i,$$

where $\mathbf{\Pi}$ is the permutation matrix. Moreover, we use this scheme for the reconnection of nodes after downsampling.

We extend our approach by considering the smoothest possible representation of the resulting sub-graph signals $\mathbf{x}_i \in \mathbb{R}^N$, whose samples are composed of the intensity values of the individual pixels, i.e. $x(k) = I(k)$ at node k for graph signal $\mathbf{x}$ on G. In particular, given the subgraph G_i, we perform a thresholding on the weights in the corresponding adjacency matrices $\mathbf{A}_i$ to obtain sparse graphs, followed by the RCM algorithm,[14] which determines the banded form of smallest possible bandwidth via a node relabelling, before computing their nearest circulant approximations.

While the primary purpose for using the RCM has been to obtain a reordered matrix (re-labelled graph) with more similar neighborhoods, whose structure is closer to that of a circulant matrix, it appears that in light of our treatment of maximum annihilation, the obtained, smallest possible bandwidth may be used for an increased sparse representation in the graph wavelet domain if the corresponding re-ordered graph signal is smooth. When the similarity measure in $\mathbf{A}_i$ is based solely on the intensity measure I of the graph signal $\mathbf{x}_i$, the relabelling obtained via the proposed approach on $\mathbf{A}_i$ converges toward performing a simple sort operation on $\mathbf{x}_i$, due to the breadth-first traversal of the RCM. We can further generalize the given subgraph to be approximated by the simple cycle, i.e. the ‘sparsest’ possible circulant graph, or alternatively, the ‘smoothest possible cycle’ in G_i, and define the sorted graph signal $\mathbf{x}_i$ on its vertices. Thereby, we obtain maximum sparsity in the graph wavelet domain by simultaneously minimizing the bandwidth of the adjacency matrix and (graph-unrelated) total variation

$$||\mathbf{x}||_{TV} = \sum_{i=2}^{N} = |x(j) - x(j-1)|$$

of the graph signal. Figure 4 illustrates the non-linear approximation performance comparing traditional methods with our proposed smoothness-inspired designs. In particular, we observe that the sparsest representation for subgraphs with generating set $S = \{1\}$ and intensity-based weights achieves the best performance by a high margin, followed by more connected, circulant approximations (*(I,sort)*, for an appropriately chosen sparsifying threshold). We also note that, while subgraph-representations with bilateral weights (*bil,RCM*) still outperform traditional methods, they are overall less effective.

6. CONCLUSION AND FURTHER DIRECTIONS

We have introduced a variety of higher-order graph wavelet constructions on circulant graphs, which can annihilate (and reproduce) polynomial graph signals, based on the fundamental annihilation property of a circulant and symmetric graph Laplacian matrix, and discussed data-driven as well as data-independent applications, where a sparse graph wavelet representation is desirable. In future work, we aim to extend the range of applications to image denoising using 'sparsifying' graph wavelets. Moreover, it would be of interest to explore additional designs of graph wavelets, which can possibly annihilate further classes of graph signals, with the aim to move beyond the current limitation of achieving the highest sparsity for the least connected graphs. Current developments include a graph-based framework for the e-spline wavelet.

REFERENCES

[1] Shuman, D. I., Narang, S. K., Frossard, P., Ortega, A., and Vandergheynst, P., "The emerging field of signal processing on graphs: Extending high-dimensional data analysis to networks and other irregular domains," *IEEE Signal Process. Mag.* **30**(3), 83–98 (2013).

[2] Coifman, R. R. and Maggioni, M., "Diffusion wavelets," *Applied and Computational Harmonic Analysis* **21**(1), 53–94 (2006).

[3] Narang, S. and Ortega, A., "Perfect reconstruction two-channel wavelet filter banks for graph structured data," *Signal Processing, IEEE Transactions on* **60**, 2786–2799 (June 2012).

[4] Hammond, D. K., Vandergheynst, P., and Gribonval, R., "Wavelets on graphs via spectral graph theory," *Applied and Computational Harmonic Analysis* **30**(2), 129 – 150 (2011).

[5] Ricaud, B., Shuman, D. I., and Vandergheynst, P., "On the sparsity of wavelet coefficients for signals on graphs," in [*SPIE Optical Engineering+ Applications*], 88581L–88581L, International Society for Optics and Photonics (2013).

[6] Ekambaram, V., Fanti, G., Ayazifar, B., and Ramchandran, K., "Circulant structures and graph signal processing," in [*IEEE International Conference on Image Processing, ICIP 2013*], 834–838 (Sept 2013).

[7] Ekambaram, V., Fanti, G., Ayazifar, B., and Ramchandran, K., "Critically-sampled perfect-reconstruction spline-wavelet filterbanks for graph signals," in [*IEEE Global Conference on Signal and Information Processing, GlobalSIP 2013*], 475–478 (Dec 2013).

[8] Kotzagiannidis, M. and Dragotti, P., "Sparse graph signal reconstruction and image processing on circulant graphs," in [*2014 IEEE Global Conference on Signal and Information Processing, GlobalSIP 2014*], 923–927 (Dec 2014).

[9] Ekambaram, V., *Graph Structured Data Viewed Through a Fourier Lens*, PhD thesis, EECS Department, University of California, Berkeley (Dec 2013).

[10] Chung, F. R. K., [*Spectral Graph Theory*], American Mathematical Society (1997).

[11] Unser, M., "Splines: A perfect fit for signal and image processing," *Signal Processing Magazine, IEEE* **16**(6), 22–38 (1999).

[12] Shi, J. and Malik, J., "Normalized cuts and image segmentation," *IEEE Transactions on Pattern Analysis and Machine Intelligence* **22**, 888–905 (1997).

[13] Chan, T. F., "An optimal circulant preconditioner for toeplitz systems," *SIAM journal on scientific and statistical computing* **9**(4), 766–771 (1988).

[14] Cuthill, E. and McKee, J., "Reducing the bandwidth of sparse symmetric matrices," in [*Proceedings of the 1969 24th National Conference*], *ACM '69*, 157–172, ACM (1969).